Impact of Surfactant Structure on Wettability and Pore-Scale Displacement Mechanisms of Non-aqueous-Phase Liquids in Heterogeneous Rocks

Gina Javanbakht

Lamia Goual

Department of Petroleum Engineering

University of Wyoming

November 9th 2016

UNIVERSITY OF WYOMING

Introduction

Contamination by nonaqueous phase liquids (*NAPLs*)

NAPLs

Light nonaqueous phase liquids (LNAPLs)	Dense nonaqueous phase liquids (DNAPLs)
• **Crude oil** • Gasoline • Benzene • Toluene	• Coal tar • Creosote • Polychlorinated biphenyl • Mercury • **Asphaltene**

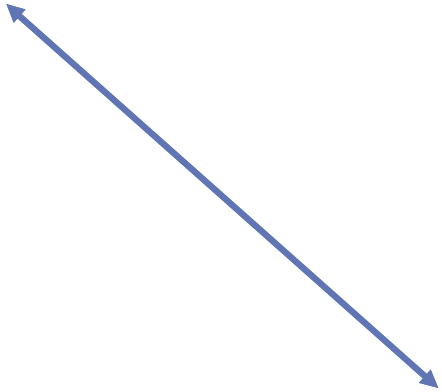

(U.S. Environmental Protection Agency, 2010)

Remediation Methods

- Water flooding
- Thermal desorption
- Pump and treat
- In situ oxidation
- Nanoremediation
- **Surfactant enhanced aquifer remediation (SEAR)**

$$P_C = \frac{2\gamma_{Brine-NAPL}\cos(\theta_{Brine-NAPL-Solid})}{r}$$

Surfactants

Hydrophilic-lipophilic balance number (HLB)

- Oil-in-water microemulsion (HLB >> 10)
- Water-in-oil microemulsion (HLB << 10)
- Middle-phase microemulsion (HLB ≈ 10)

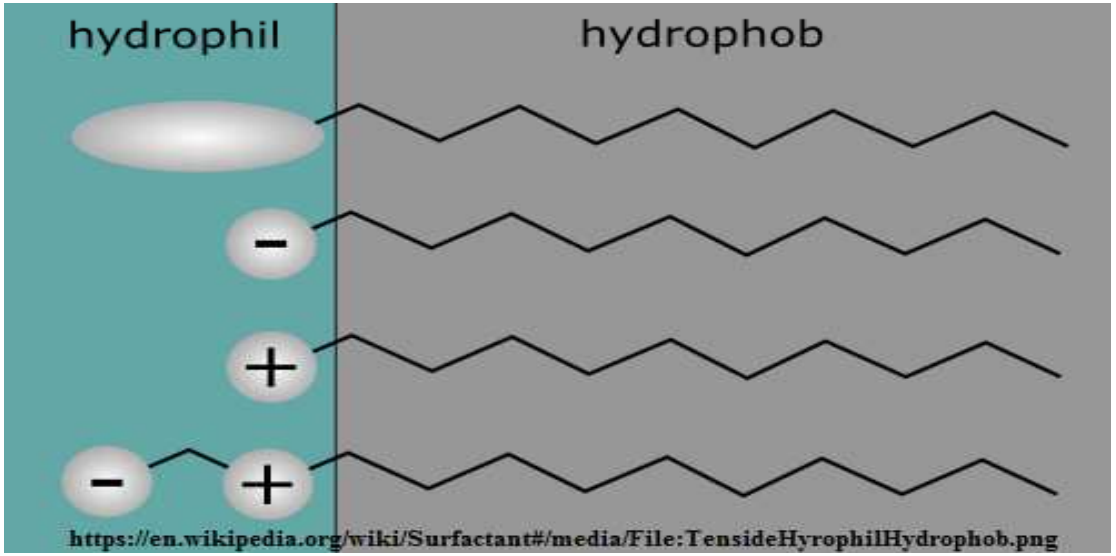

Microemulsion Phases Formed by Surfactant

O/W(Winsor type I) Winsor type III W/O(Winsor type II)

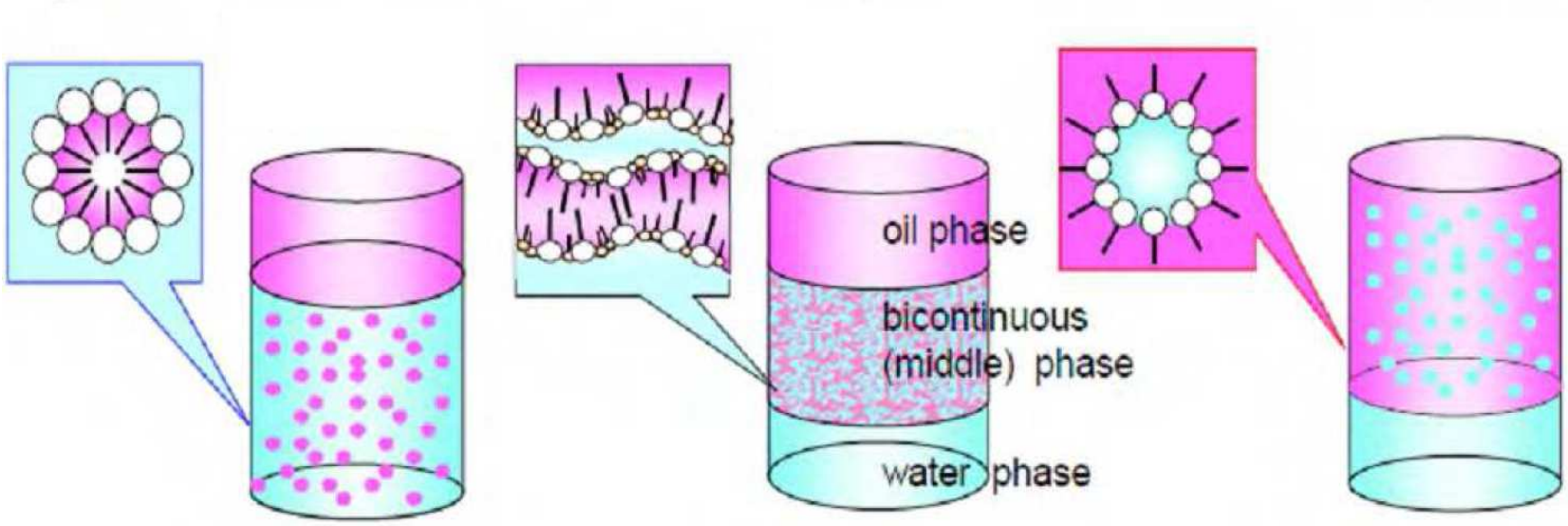

Hydrophil > lipophil Hydrophil = lipophil Hydrophil < lipophil

Removal Mechanisms

- Mobilization

Desirable in aquifer contaminated by LNAPLs

- Micellar solubilization

Solubilize adsorbed DNAPLs (i.e., asphaltenes)

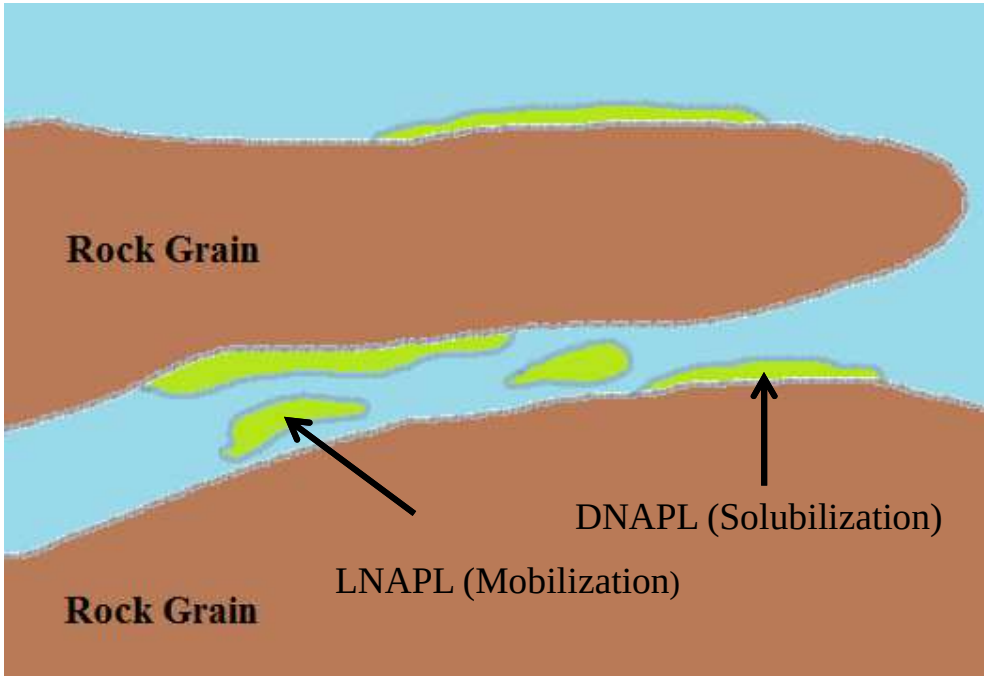

Javanbakht, G.; Goual, L. Mobilization and Micellar Solubilization of NAPL Contaminants in Aquifer Rocks. *Journal of Contaminant Hydrology* **2016**, *185–186*, 61–73.

Materials and Methods

Rock

Fountain formation, a heterogeneous Pennsylvanian sedimentary rock consisting primarily of Conglomerate, Sandstone, or Arkose formed from the Sherman Granite.

Porosity: 12-15%

Permeability: 2-5 mD

NAPL

NAPL is Milne point crude oil from Alaska

NAPL	
ϱ^{20C} (g/mL)	0.9214
Reflective Index at 20°C	1.5222
Viscosity (mPa.s)	112.0
C (%)	85.07
H (%)	7.75
N (%)	1.09
O (%)	1.61
S (%)	4.63
H/C	1.1
Asphaltenes (wt%)	9.03
TAN (mg of KOH/g)	1.69
TBN (mg of KOH/g)	2.25
TBN/TAN	1.33

Surfactants

- **Alkyl polyglucosides** : (n-Dodecyl β-D-Maltoside) nonionic, sugar based environmental friendly

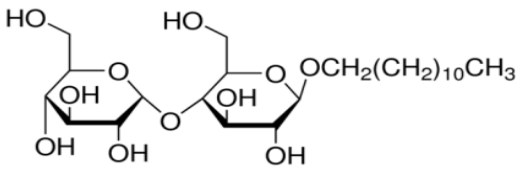

- **Alkyl phenyl ethoxylates** : (Triton X-100) nonionic, environmental friendly with a branched-alkyl chain tail

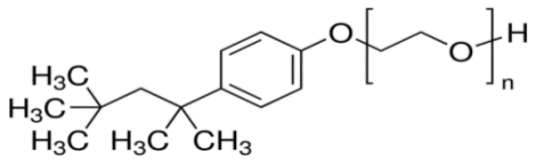

- **Alkyl ethoxylates** : (Bio-Soft N1-7) linear alcohol alcoxylates , nonionic, and environmental friendly

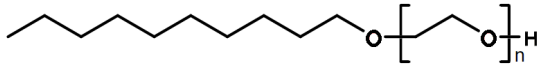

- **Biosurfactants** : (Saponin) nonionic, and environmental friendly with complex structure

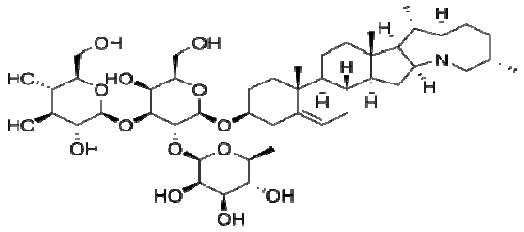

Surfactants (Cont'd)

Name	Structure	Chemical formula	MW (gr/mol)	HLB	CMC (wt%)
n-Dodecyl β-D-Maltoside	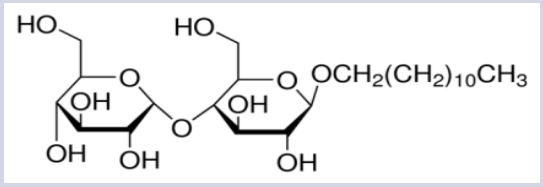	$C_{24}H_{46}O_{11}$	511	13.35	0.02
Bio-Soft N1-7	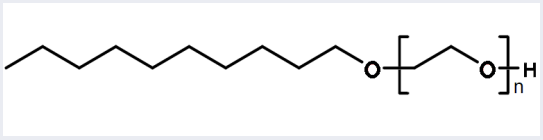	$H_3(CH_2)_{10}$-$O(CH_2CH_2O)_7H$	647	12.9	0.01
Triton X-100	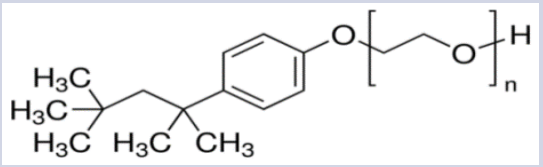	C14H22O(C2H4O)10H	625	13.5	0.02
Saponin	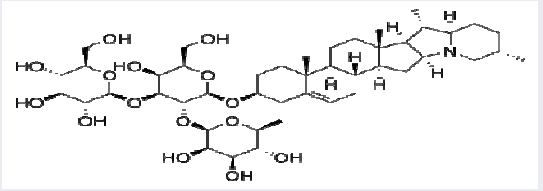	$C_{45}H_{73}NO_{15}$	1650	36.3	0.01

Experimental Setup and Procedure

Rock Mineralogy

- Scanning electron microscopy (SEM) images and energy dispersive X-ray analysis spectroscopy element maps
- Transmission micro-CT scanner (3D high-resolution map of pore space)

Scanning electron microscopy

Micro-CT scanner

Phase Behavior

Brine solution (0.2 wt% surfactant in brine) and NAPLs at a volume ratio of 1:1 were shaken for 1 hour with a speed of 300 strokes/minute and then rested for two days at 25 °C and atmospheric pressure

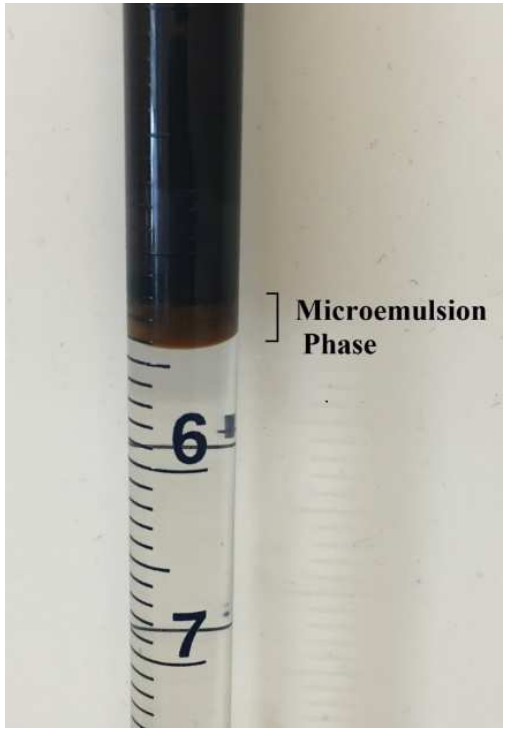

High Resolution Transmission Electron Microscopy (HRTEM)

O/w microemulsions extracted from the rag layer between NAPL and diluted brine

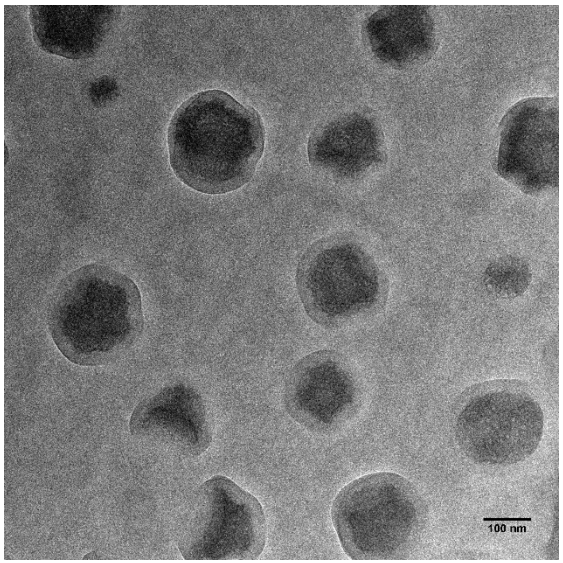

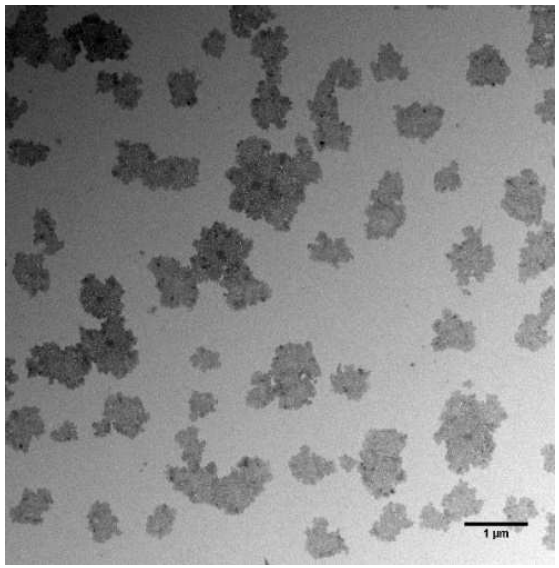

Microemulsions

Interfacial Tension

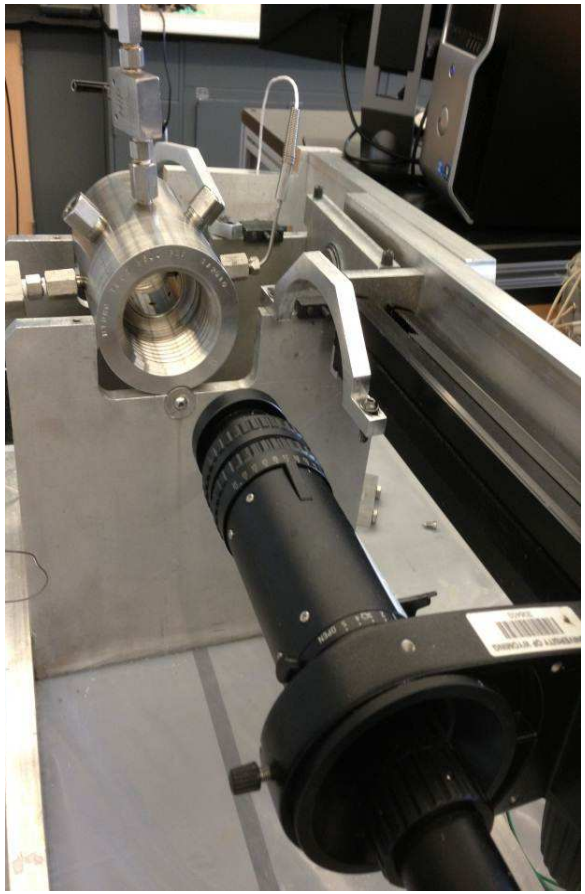

Experimental set up

Rising/captive bubble
Tensiometry for high IFTs

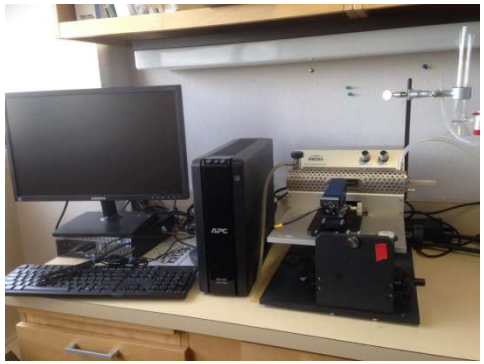

Spinning drop tensiometry
for low IFTs

Contact Angle

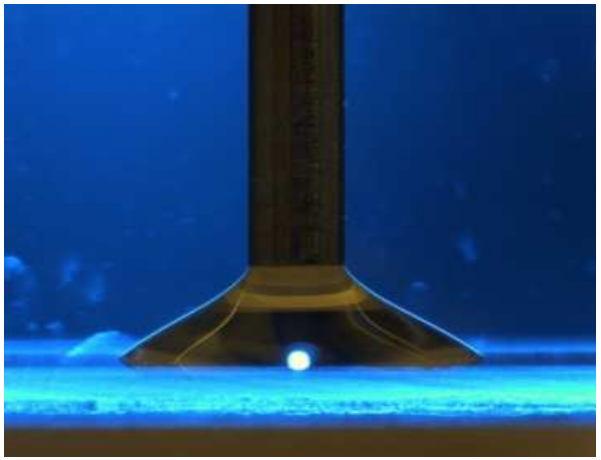

Dynamic CA on clean quartz

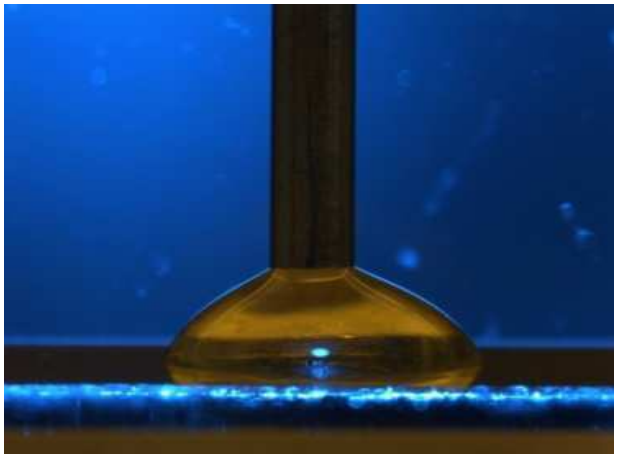

Dynamic CA on contaminated quartz

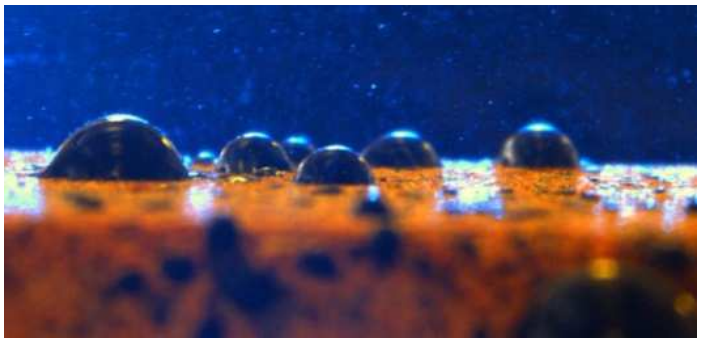

Static CA measurements during spontaneous imbibition

Spontaneous Imbibition

Arkose core sample
(38 × 50.8 mm)

Vacuum pump and cell
(100% water saturation)

Spontaneous Imbibition (Cont'd)

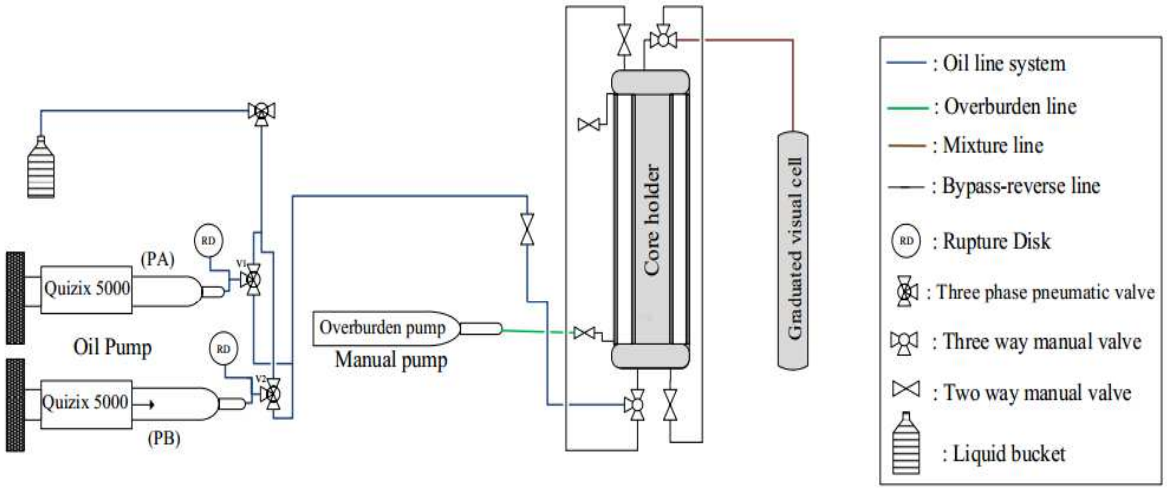

Core flooding system
(50% NAPL saturation)

Amott imbibition cells

Results and Discussions

Rock Characterization

Arkose minerals

- Feldspar and clay (78.5%)
- Quartz (14.2%)
- Calcite (7.0%)
- Muscovite (0.3%)

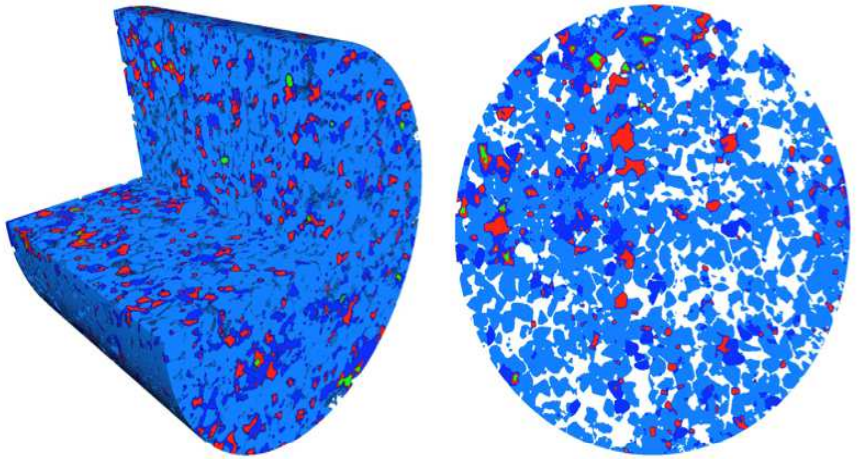

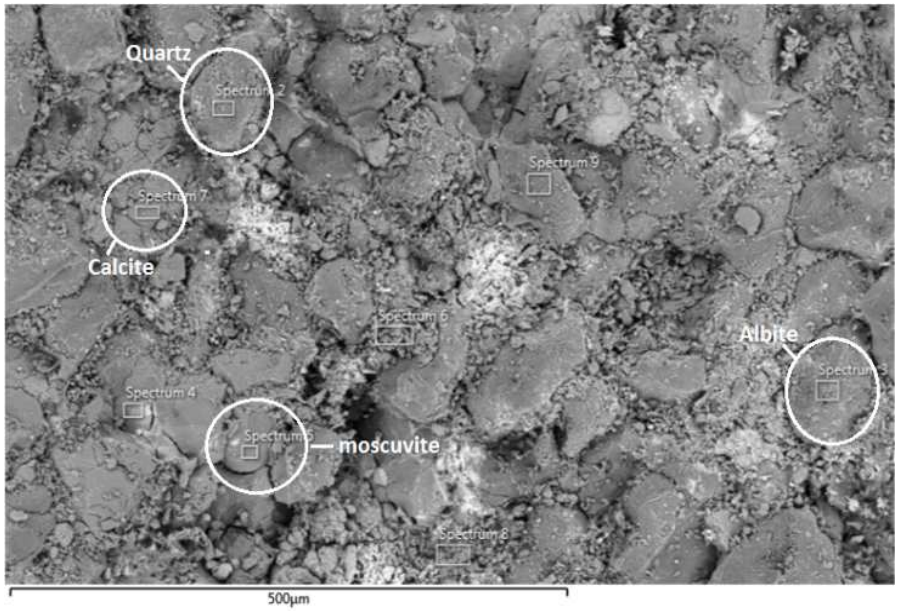

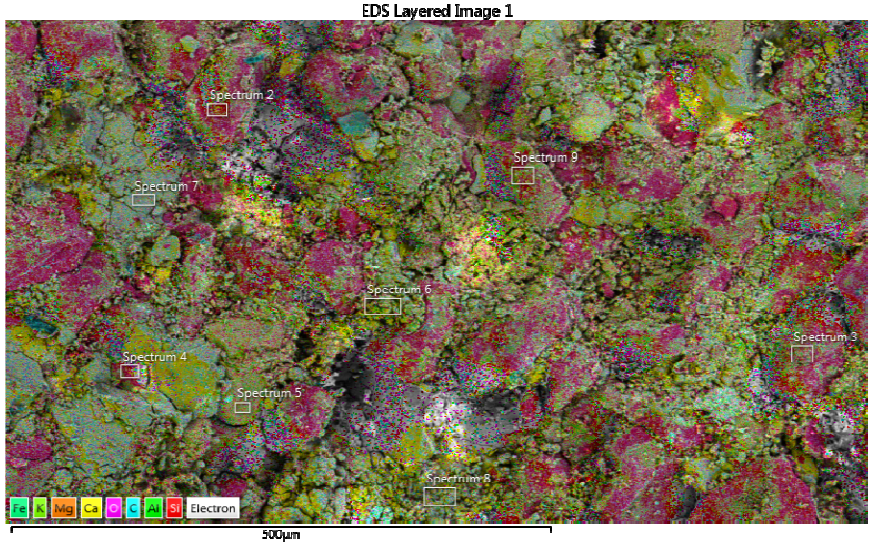

Phase Behavior

Surfactants formed Winsor type III microemulsion phase with NAPL

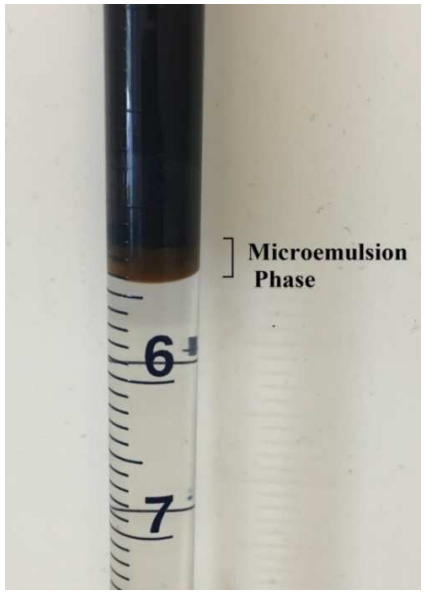

n-Dodecyl β-D-maltoside

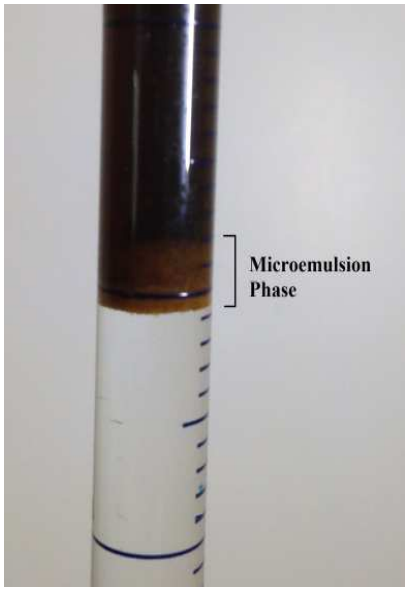

Bio-soft N1-7

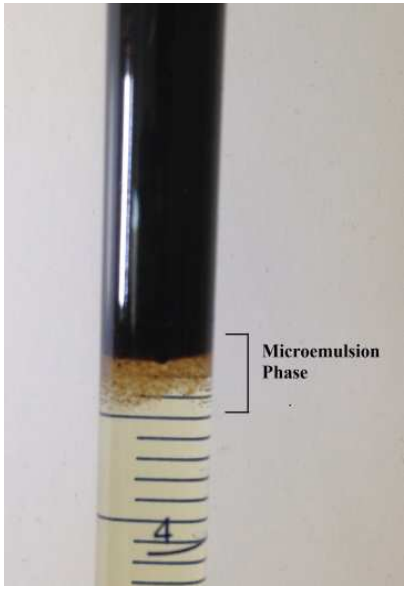

Triton X-100

Saponin

HRTEM Imaging

n-Dodecyl β-D-maltoside

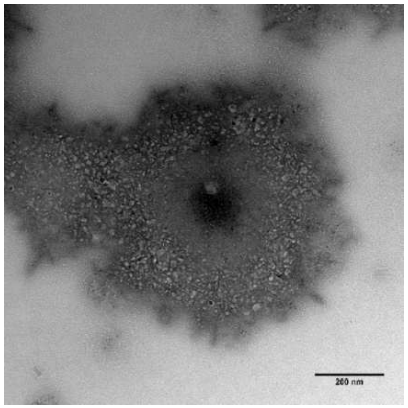

800 nm

N1-7

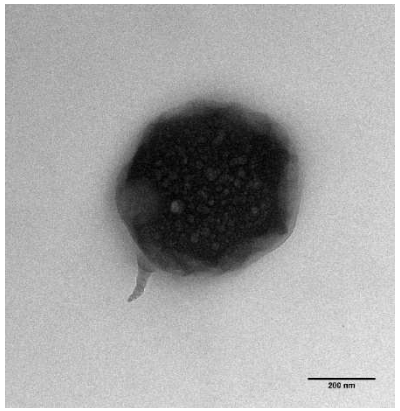

400 nm

Triton X-100

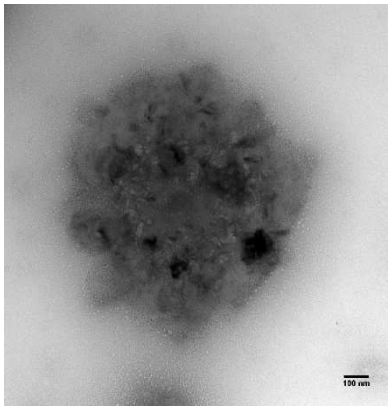

800 nm

Saponin

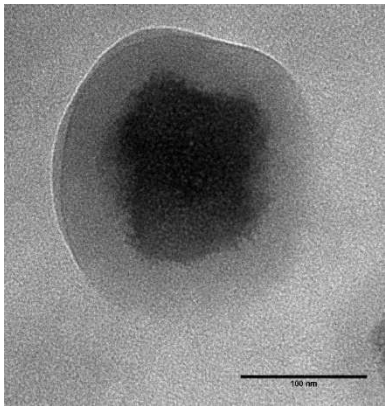

200 nm

Aged Saponin

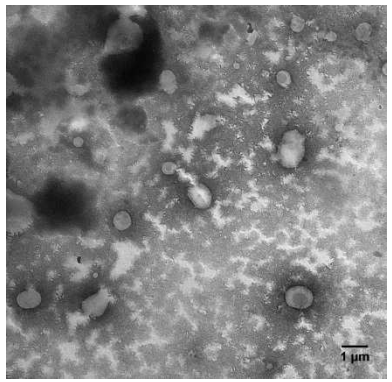

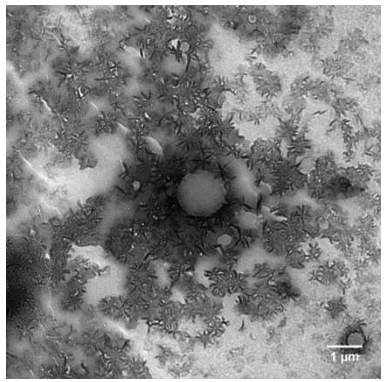

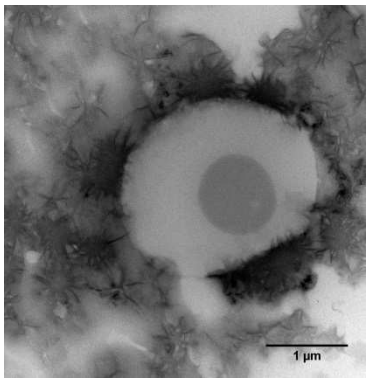

> 1 micron

Interfacial Tension

MEs promote mobilization by increasing the capillary number

$$Ca = \frac{\mu V}{\Upsilon}$$

NAPL/brine IFT : 22.5 mN/m

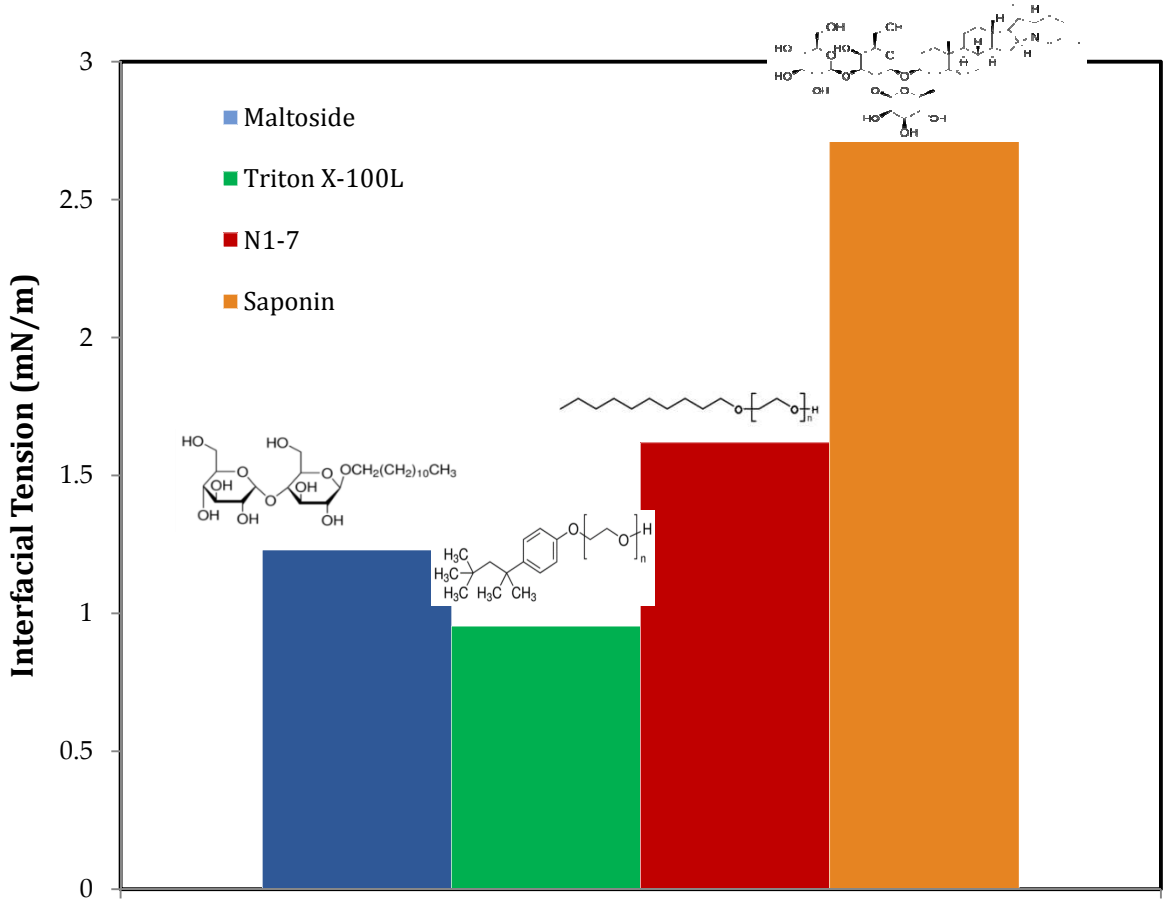

Contact Angle (Cont'd)

- Surfactant alters the wettability of contaminated rock surfaces from weakly-water wet back to water-wet
- The adsorption of surfactant molecules via their hydrophobic tails on the thin NAPL layer causes asphaltene molecules to detach and form Winsor Type I microemulsions

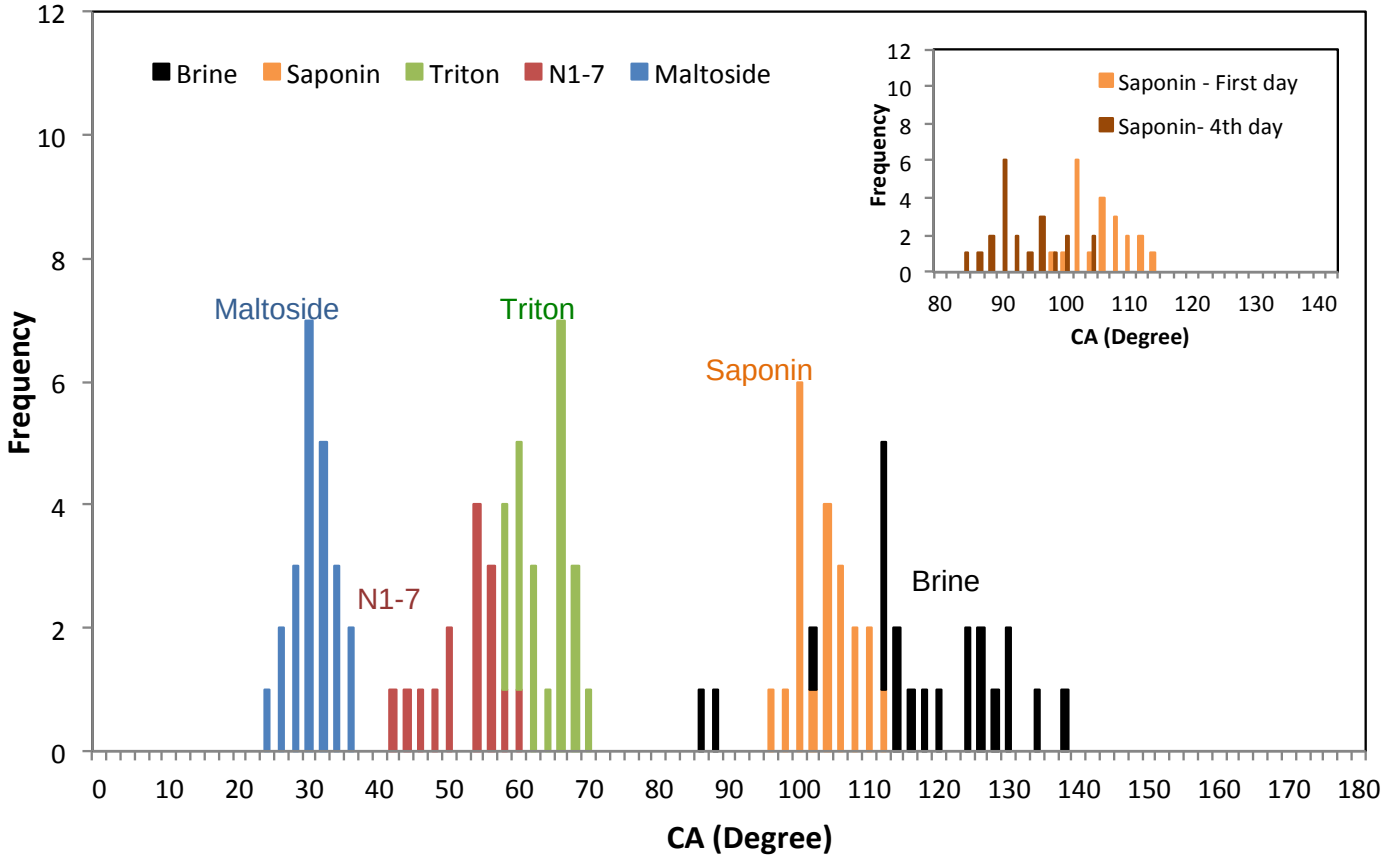

Spontaneous Imbibition

Solubilization vs. Mobilization

Effect of surfactant (maltoside)-in-brine on NAPL removal from Arkose core samples containing 50% water and 50% NAPL

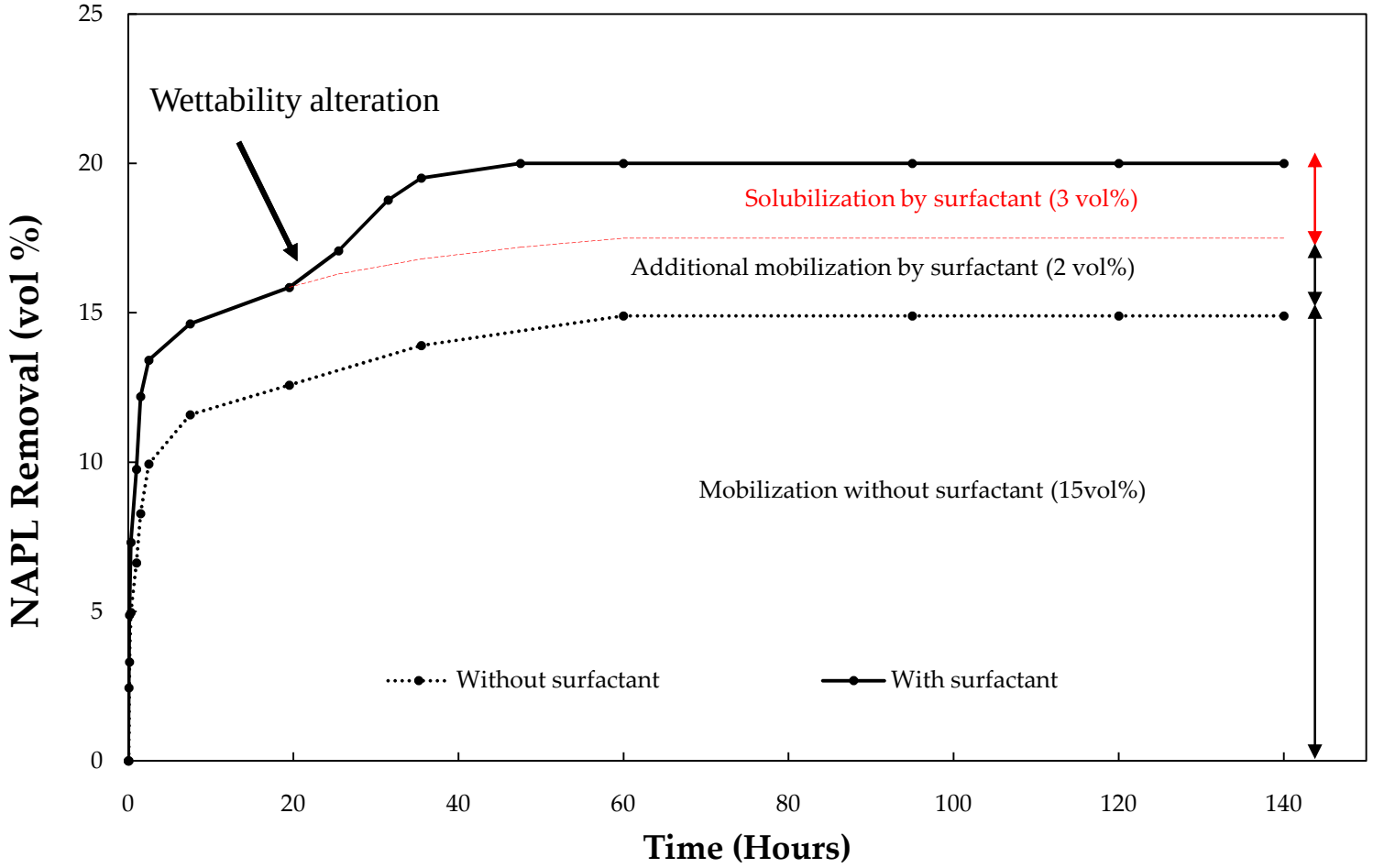

Thin Sections Analysis

- The channels that contained dolomite cement were remained contaminated after surfactant treatment
- Surface roughness plays an important role in wettability alteration

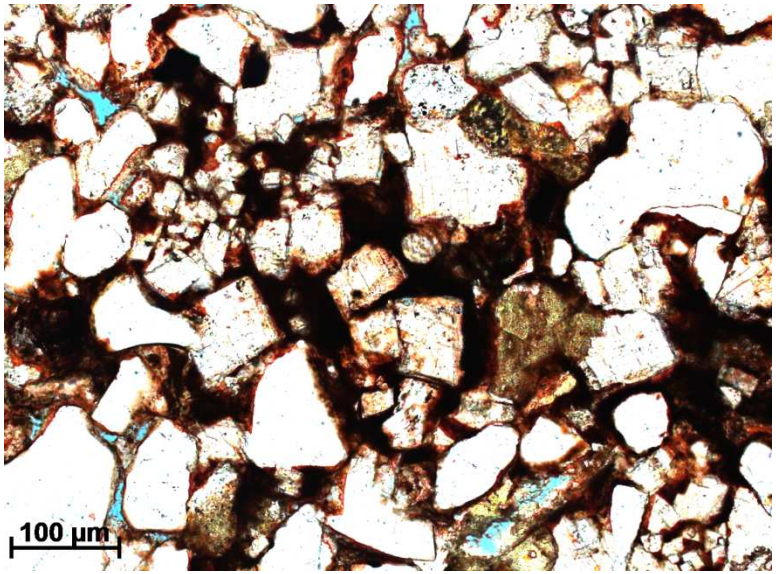

Without surfactant

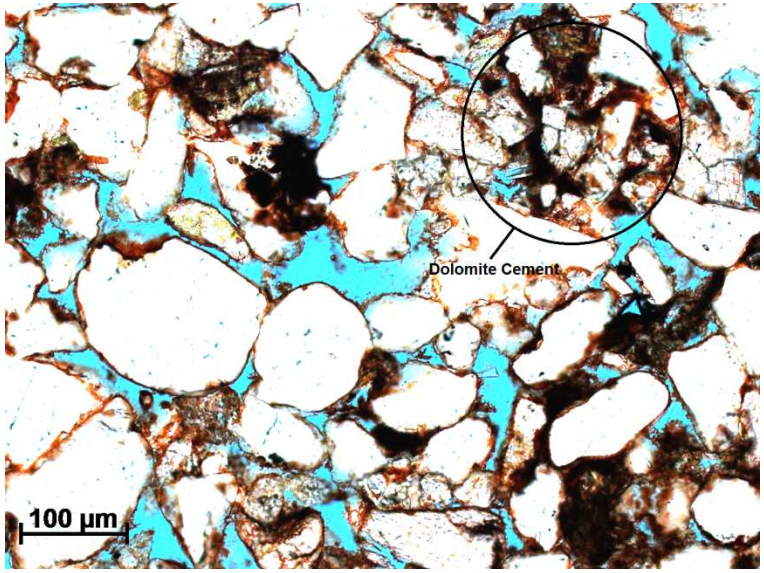

With *n*-dodecyl β-D-maltoside

Conclusions (Cont'd)

- Surfactant self-assembly reduces the NAPL mobilization rate especially in low permeability rocks

- This work suggest that mixtures of surfactants with two structural types can promote both mobilization and micellar solubilization of NAPL in porous media. Type 1 contains a linear tail and a large hydrogen-bonding head, whereas type 2 has a highly branched tail and a smaller hydrogen-bonding head.

- References:

- "Mobilization and Micellar Solubilization of NAPL Contaminants in Aquifer Rocks" Javanbakht, G.; Goual, L. *Journal of Contaminant Hydrology* **2016**, *185–186*, 61–73.

- "Impact of Surfactant Structure on NAPL Mobilization and Solubilization in Porous Media." Javanbakht, G.; Goual, L. *Ind. Eng. Chem. Res.* **2016**.

Acknowledgements

We gratefully acknowledge financial support of

- National Science Foundation (CAREER Award # 1351296)
- HESS Corporation

Thank you

Questions?

Spontaneous Imbibition

Spreading behavior of produced NAPL

$$S = \gamma_{g/w} - \gamma_{g/o} - \gamma_{w/o}$$

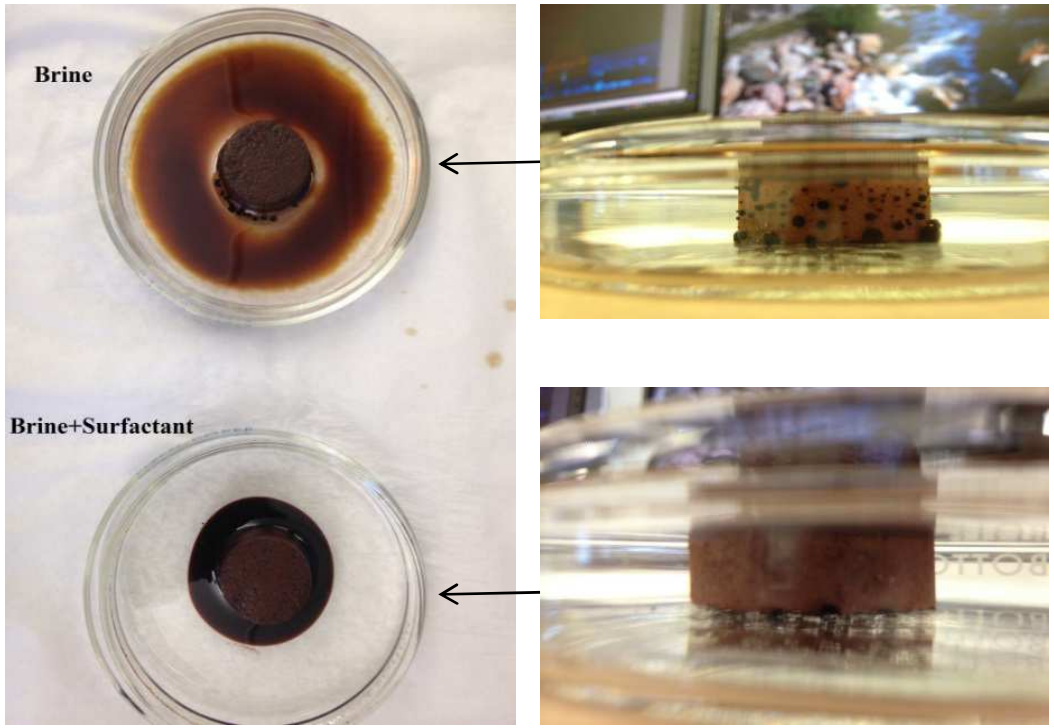

HRTEM

Tecnai TF20 S-Twin High Resolution Transmission Electron Microscope (HRTEM) from FEI. The microscope features a TIETZ F415MP 4k × 4k multiport CCD camera with a 4-port readout and 15 μm pixel size. Two types of samples were prepared on silicon dioxide custom coated carbon TEM grids from SPI Supplies. The first sample contained surfactant micelles obtained by mixing 0.2 wt% of surfactant in brine. The second sample consisted of o/w microemulsions prepared by extracting a small amount of the rag layer between NAPL and brine. Because the rag layer phase was too thick to image under microscope, it was diluted 40 times in the same brine. All samples were imaged by the microscope at 200 kV accelerating voltage under bright field illumination mode. Image J software was used for processing the images to measure the average size of the micelles and microemulsions particles.

CA

- The thin brine film between NAPL and mineral surface becomes unstable and collapses because of weak DLVO forces and more dominant electrostatic and van der Waals forces.The collapse of the brine film allows asphaltenes to adsorb onto the mineral surface and alter its wettability.
- The contact angles were smaller since NAPL 2 is less basic than NAPL 1, thus there is less electrostatic repulsion between Ca^{2+} ions of brine and dissociated basic groups of NAPL.

CT- scanner

To determine the abundance of each mineral, a rock sample was placed in a miniature Hassler type core holder made of carbon fiber and imaged at high resolution using a transmission micro-CT scanner (VersaXRM-500, Zeiss). The X-ray source was operated at a voltage of 60 kV and a power of 5 W. The 3D map of pore space was reconstructed based on 2000 projections with an angular coverage from -104° to 104° and an angular step size of 0.104°. For each projection, 5 s step (exposure + motion) and 3 s exposure (dwell) time were used. Each projection is a 2030×2030 pixel image with a resolution of 2.02 microns per pixel. Reconstruction of the projections with an appropriate center shift value gave the 3D high-resolution map of the pore space shown in. A binary voxel map of the pore space was then generated using Avizo Fire 8.0 visualization and analysis software. The non-local means filter was applied to smoothen the raw data and reduce noises. The intensity ranges for different minerals were determined by applying the interactive thresholding tool of Avizo software. The Edit new label field tool was used to assign each intensity range to each mineral.

Brine

Cation	Concentration (ppm)
Al^{+3}	0.116
B^{+3}	3.031
Ca^{+}	**20.43**
Cu^{+2}	0.022
Fe^{+2}	0.078
K^{+1}	2.868
Mg^{+2}	0.445
Mn^{+2}	0.007
Na^{+1}	3.609

1 M $CaCl_2$

CMC
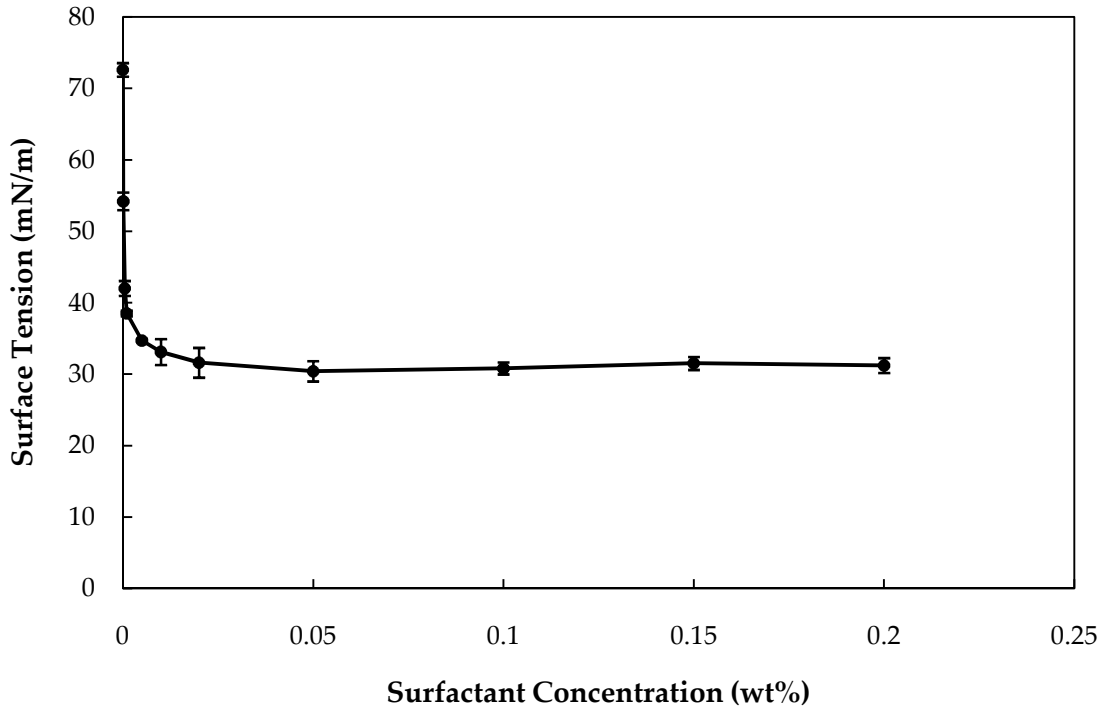
- Effect of surfactant concentration on surface tension
- CMC point of surfactant (low CMC)